

Generic Linking of Finite Element Models for Non-Linear Static and Global Dynamic Analyses of Aircraft Structures

A.J. de Wit¹, D. Akçay Perdahcioğlu², T. Ludwig³
W.M. van den Brink¹ and A. de Boer²

Abstract: Depending on the type of analysis, Finite Element (FE) models of different fidelity are necessary. Creating these models manually is a labor intensive task. This paper discusses two approaches for generating FE models of different fidelity from a single reference FE model. The models are created with a single modelling and meshing toolkit. These different fidelity models are created for use with global-local non-linear static analysis and for use with dynamic linear sub-structuring reduction method. Efficiency of the developed approaches is demonstrated via non-linear static and modal analysis of a carbon-fiber stiffened panel.

Keywords: global-local, sub-structuring and reduction, FEA, coupling

1 Introduction

During take-off, flight and landing, an aircraft structure experiences different kind of loading conditions, such as pressure loads, thermal loads, dynamic loads, and so on. One approach to determine the structural responses due to these external loads is using the Finite Element (FE) method. Typically, each loading condition imposes different fidelity requirements to the FE model and utilizing the same model for the analysis may not be computationally efficient. Therefore, different fidelity models have to be constructed, and data is transferred from the low-fidelity to the high fidelity model and vice versa. Throughout the text the low-fidelity model is called global model and the high-fidelity model is called local model. The manual set up of local models and the transfer of data is a time consuming process. A procedure that takes over (parts) of the manual process of creating analysis models and transfer of data has the potential of significantly reducing development times.

¹ National Aerospace Laboratory - NLR, Collaborative Engineering Systems Department, the Netherlands, adewit@nlr.nl, brinkw@nlr.nl

² University of Twente, Faculty of Engineering Technology, the Netherlands, d.akcay@ctw.utwente.nl

³ SMR Engineering and & Development, Switzerland, T.Ludwig@smr.ch

The objective of the present work is to reduce the time consuming task of manually generating different fidelity models from a given structural coarse global FE model using an automated approach. Thereby, details can be automatically added or extracted to/from the global model depending on the analysis that has to be performed. This way, manual creation and coupling of different fidelity models is replaced for an efficient automated approach.

This research focuses on two relevant use cases where the engineer encounters the issue of creating a detailed model from a global model and couples the two models for subsequent analysis. The first case is after a global non-linear static analysis has finished and a closer look within certain areas of the global model is desired. In these areas, an extensive local analysis is necessary. In industry, this is called an un-folding analysis. Contrary to industrial practice, in this work the results of the local analysis are transferred back to the global analysis, this is commonly referred to as kinematic coupling. The second case is when a global dynamic analysis has been carried out and small changes in e.g. stiffness in the initial model require a second analysis to compute the global dynamic response. In this paper, an automated approach is presented to reduce the modelling efforts associated with inclusion of local detailed FE models into a global FE model.

This paper is organized as follows: In the second section, the nonlinear global-local analysis is described. The third section covers a sub-structuring and reduction method targeted at modal analysis. The two methodologies are demonstrated on a carbon-fiber stiffened panel in the fourth section. Finally, in the fifth section, the conclusions and the directions for future work are given.

2 Global-local analysis and tight two-way coupling methodology

2.1 Methodology

A global-local analysis consists of an initial phase analyzing the entire structure via a global model, discarding details that may have no significant contribution to the structures' overall behavior. After the global analysis is completed, a cut-out is made in the global model at locations where a closer look at the local behavior of structural details is required, such as e.g. stringer-skin bonding area of a stiffened panel. The loads computed from the global model on the cut-out section are then transferred to boundary and/or loading conditions of a local model. In industry this procedure is called unfolding analysis.

Because the analysis of local models often reveals changes in stiffness and stability that might affect the global model response, it is desired to map those changes back to the global model. This can be achieved by tuning the global FE model to match the stiffness of the local models, but it is an iterative process involving man-

ual work. To simplify and to speed up this task, techniques such as the hierarchical superposition analysis have been developed to provide an accurate and computationally efficient means to include detailed physical behavior into a coarse scale model. An overview of different approaches is presented in (Fish and Shek, 2000). In the present paper, there are only two scales: A large scale which is referred to as global, and a smaller scale is referred to as local.

Variational multi-scale frameworks such as (Hund, 2007) that involve an additive split between the global and local displacements, $u = \bar{u} + u'$, are not directly suited to geometric nonlinear analysis: The complete elimination of rigid-body motions from the gradient deformation tensor F cannot be performed independently on the global and local scales, as the polar decomposition theorem $F = RU$ does not hold for sums (R being the rotation tensor and U the right stretch tensor):

$$RU = F = \bar{F} + F' = \bar{R}\bar{U} + R'U' \quad ; \quad U \neq \bar{U} + U' \quad (1)$$

To amend this, a co-rotational framework may be used. In the present work however, the global contributions to the vector of internal forces (first variation) and to the stiffness matrix (second variation) are eliminated in the regions where local elements are present, and the global and local sub-domains are kinematically coupled. Compared to a co-rotational approach, the relative sizes of global and local elements can be chosen arbitrarily, because the rigid-body motions are always eliminated exactly and all elements make use of the Total-Lagrangian formulation. This setting and the nomenclature that will be used in the following are illustrated in Figure 1. The subscript 1 denotes the degrees of freedom (d.o.f.) of the global FE model that are not connected to the local FE model(s), and 2 the d.o.f. of the global FE model that are connected to the local FE model(s). The subscript 3 denotes the d.o.f. of the local FE model(s) that are connected to the global FE model, and 4 the remaining d.o.f. of local FE model(s). The kinematic coupling operates on the d.o.f. of the interfaces Γ_2 and Γ_3 .

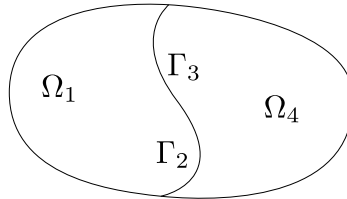


Figure 1: Schematic representation of global sub-domain Ω_1 , global part of interface Γ_2 , local part of interface Γ_3 , and local sub-domain Ω_4 .

2.2 Criteria for insertion of local models

When local FE models should be inserted automatically into the global FE model, a criterion is necessary that will mark a region within a global model to create and superimpose a local model. In the present study, a Hashin (Hashin, 1980) failure criterion is chosen to mark finite elements in the global model critical. Subsequently, the critical finite elements exceeding the maximum allowable failure index are used to determine the size and shape of the local model.

The Hashin failure criterion is mesh dependent. Therefore, the size of the area to be extended depends on the mesh density of the global model. An alternative approach is to extend entire pre-defined regions of the global FE model via a local model whenever one or more elements in those regions are marked critical. In this case, the local models cover the same area of the global model for different global mesh densities, with the drawback of obtaining local models that are likely to be larger and to have more degrees of freedom (d.o.f.) than necessary.

2.3 Sub modelling framework

In contrast to mesh-refinement methods, global-local analysis imposes higher requirements on the created FE models, resulting in a higher pre-processing effort. But in industry, it is not only important that FE analysis produces results accurately and reliably, but in addition that the amount of manual work to create and maintain the FE models is kept to a minimum. The sub modelling framework addresses this problem as it allows to specify a common CAD surface geometry and a common set of material properties, from which global shell and local volume FE models can be created automatically, including the local/global mapping.

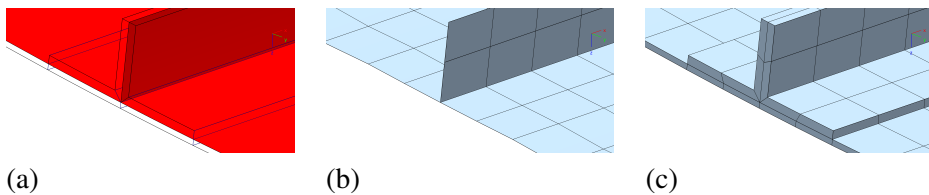


Figure 2: (a) CAD surface geometry of skin and stringer intersection. (b) Shell element model of a skin and stringer intersection. An offset is necessary for the shell elements located at the stringer foot to model the skin-foot area via a single layer of shell elements.

(c) Solid element model of the skin and stringer intersection showing the skin-foot area modelled with two stacked volume elements.

Shell FE models of skin stringer junctions typically combine the stringer foot and the skin beneath in a single set of shell elements, and the reference surface if off-

set accordingly. This way, the number of shell elements with offsets is kept to a minimum, which is desirable in view of the reduced numerical effectiveness of offset shell elements. For skin stringer junctions such as the one shown in Figure 2, the sub modelling framework automatically creates shell FE models with this modelling technique, as well as the matching volume FE models.

The sub modelling framework is written in Python (Python Software Foundation, 2012) and creates input files containing the nodes and the finite element connectivity list for the B2000++ pre-processor. It is steered with Python scripts to define the CAD surface geometry and to set parameters such as the desired mesh density.

2.4 Kinematic coupling between global and local FE models

The numerical formulation and the implementation are greatly simplified by imposing the condition that any local element must be fully contained within a single global element. With this condition, local element boundaries cannot cross global element boundaries. Instead, some of the local element boundaries coincide with the global element boundaries, and some of the local nodes coincide with the global nodes.

Contrary to the work of Hund (Hund, 2007) where global and local models consist of membrane elements, in the present study, the global model consists of shell elements and the local models consist of 3D volume elements. To couple the global analysis to the local analysis, a linking/mapping between the local and global model is necessary. This is achieved as follows: Every FE node within the local model must have a reference in the global model. This reference is constructed in terms of the natural element coordinates of the global element. A straightforward mapping for a single global element is shown in Figure 3(a), where all local nodes are assigned global natural boundary coordinates for one single global element.

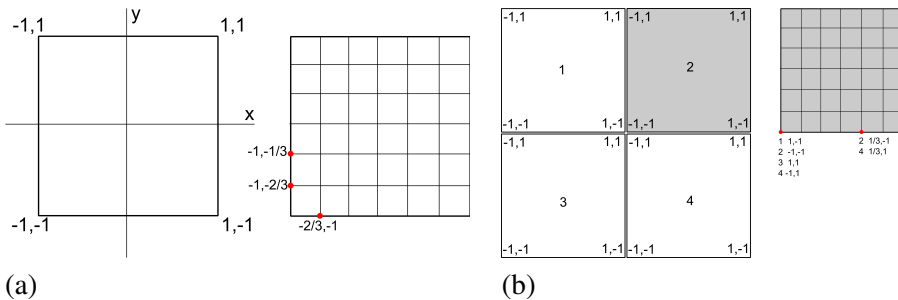


Figure 3: (a) Linking nodes of local elements to a single global element. Local nodes expressed in global element natural coordinates. (b) Linking nodes of local elements to multiple global elements.

If a local model is connected to multiple global elements, the linking is constructed for each global element to which the local model nodes are connected, see Figure 3(b).

The global shell elements are based on first-order shear deformation theory where the shell element fibre normals – and thus the shell element sides – remain straight under deformation. Thus, local element boundaries that coincide with global element sides must remain straight, too, and applying a constraint merely to the local nodes coinciding with the shell reference surface, see Figure 4(a), is not sufficient. As shown in Figure 4(b), the 3D volume element sides do not deform properly. To amend this problem, all nodes of local element boundaries that coincide with global element boundaries are constrained such that they follow the shell element deformation, see Figure 4(c).

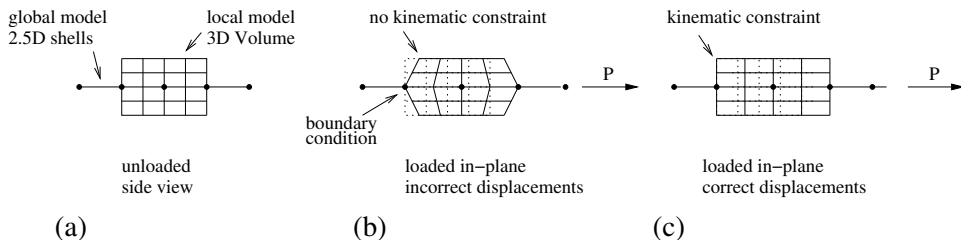


Figure 4: Kinematic constraints are applied to keep the boundaries of the local 3D model in line with the global shell element model. (a) A 2D side view of a shell element model (line) and volume element model (rectangular grid) superimposed. (b) If a force is applied to the shell element model the volume element model does not deform correctly. (c) A remedy is to constrain the nodes of the local volume model that coincide with the boundaries of global shell elements to remain on those shell element boundaries.

Due to the plane stress condition of first order shear deformation theory, volume elements will be overconstrained for materials where the Poisson number is nonzero in the normal direction, possibly resulting in undesirable stress concentrations. This problem can be mitigated by using an orthotropic material definition for the volume elements where the Poisson number for the normal direction is set to zero. However, a true 3D stress state in the local elements cannot be achieved in this way.

To obtain the constraints, the shell element shape functions and their derivatives must be evaluated at the positions of the adjacent volume element nodes, using the mapping between the local and the global model. Due to the rotational d.o.f., these constraints are nonlinear, as they depend on the applied deformation field.

The d.o.f. of local nodes that coincide with global nodes are redundant and must be suppressed, otherwise, the global stiffness matrix will become singular.

2.5 Sparse matrix factorization and static condensation

In quasi-static nonlinear analysis, for each load increment, several Newton iterations are performed until the norm of the vector of internal forces falls below a user-defined threshold and the iterations are considered converged. The full Newton method is appropriate when the problem is highly nonlinear such as in the post-buckling regime. For each Newton iteration, the tangent stiffness matrix is factorized, and a back-substitution with the vector of internal forces is performed to obtain the correction vector of the d.o.f.. The factorization and back-substitution can be performed with a sparse direct matrix solver, such as the MUMPS package, see (Amestoy, Duff, Koster, and L'Excellent, 2001), and (Amestoy, Guermouche, L'Excellent, and Pralet, 2006). Direct solvers are more robust than iterative solvers, which is particularly important in post-buckling analysis.

Sparse direct matrix solvers exploit the generally high sparsity of the tangent stiffness matrix and achieve higher computational efficiency than full direct solvers, but require a symbolic factorization step prior to the actual factorization. Symbolic factorization determines the structure of the tangent stiffness matrix and must be performed only when the structure changes, for instance, when new local elements are added.

Since the symbolic factorization has a considerable computational overhead, it is desirable to keep the structure of the tangent stiffness matrix constant. Further, many FE solvers, including the B2000++ nonlinear quasi-static solver, are implemented on the assumption that the number of d.o.f. of the FE model to be analyzed remains constant during the analysis.

These requirements can be fulfilled by defining the local FE model(s) prior to the analysis and keep them during the whole analysis. This way, the overhead of symbolic factorization is negligible as it has to be carried out only once. Alternatively, the local FE model(s) can be statically condensed into the global FE model, such that the structure of the condensed system of equations does not depend on the local FE model(s). The latter approach offers more flexibility and is described in the following.

Let K_{ij} the stiffness sub-matrix associated with sub-domains i and j . With the linearized kinematic coupling constraints $u_2 C + u_3 = 0$ the system of equations can be written as follows:

$$\begin{pmatrix} K_{11} & K_{12} & 0 & 0 & 0 \\ K_{12}^T & K_{22} & C & 0 & 0 \\ 0 & C^T & 0 & I & 0 \\ 0 & 0 & I & K_{33} & K_{34} \\ 0 & 0 & 0 & K_{34}^T & K_{44} \end{pmatrix} \begin{pmatrix} \Delta u_1 \\ \Delta u_2 \\ \Delta \lambda \\ \Delta u_3 \\ \Delta u_4 \end{pmatrix} = \begin{pmatrix} r_1 \\ r_2 \\ r_\lambda \\ r_3 \\ r_4 \end{pmatrix} \quad (2)$$

with Δu denoting the corrections of the d.o.f. and r the residual forces.

The system (2) could be solved as a whole. Conversely, with static condensation, one obtains the following system of equations:

$$\begin{pmatrix} K_{11} & K_{12} & 0 & 0 \\ K_{12}^T & K_{22} & C & 0 \\ 0 & C^T & 0 & I \\ 0 & 0 & I & \tilde{K}_{33} \end{pmatrix} \begin{pmatrix} \Delta u_1 \\ \Delta u_2 \\ \Delta \lambda \\ \Delta \tilde{u}_3 \end{pmatrix} = \begin{pmatrix} r_1 \\ r_2 \\ r_\lambda \\ \tilde{r}_3 \end{pmatrix} \quad (3)$$

with the Schur matrix

$$\tilde{K}_{33} = K_{33} - K_{34}K_{44}^{-1}K_{34}^T \quad (4)$$

In general, the Schur matrix \tilde{K}_{33} is so dense that it can be considered a full sub-matrix in the system (3), whose structure thus becomes independent of the local FE model(s). This way, during nonlinear analysis, frequent changes to the local FE model(s) are possible without having to re-perform symbolic factorization. In the view of the authors, this is the principal advantage of static condensation in this context.

While the term $K_{44}^{-1}K_{34}^T$ of equation (4) can be computed efficiently using sparse-matrix factorization for K_{44} and back-substitution with K_{34}^T , in the present implementation, the pre-multiplication of this term with K_{34} is performed as a dense matrix-matrix multiplication: The implementation of sparse matrix-matrix multiplication would entail the same difficulties as the implementation of a sparse solver. Therefore, this operation is not as effective as it could be, as the computational complexity is $O(n_3^2 n_4)$, where n_3 is the number of local d.o.f. at the interface, and n_4 is the number of internal degrees of freedom. It is worth noting that the MUMPS solver supports a more effective computation of the Schur matrix.

To consider the Schur matrix as a full matrix allows the nonlinear kinematic coupling constraints to be implemented by reduction rather than with Lagrange multipliers, thereby eliminating the d.o.f. of sub-domain Γ_3 and yielding a further-reduced system of linearized equations:

$$\begin{pmatrix} K_{11} & K_{12} \\ K_{12}^T & \hat{K}_{22} \end{pmatrix} \begin{pmatrix} \Delta u_1 \\ \Delta \hat{u}_2 \end{pmatrix} = \begin{pmatrix} r_1 \\ \hat{r}_2 \end{pmatrix} \quad (5)$$

Here, the sub-matrix \hat{K}_{22} contains the contributions of the local FE model(s) and is considered a full matrix. Thus, the structure of the system (5) is independent of the local FE model(s).

2.6 Implementation of kinematic coupling and static condensation in B2000++

For the nonlinear solution procedure, the existing quasi-static nonlinear solver is used together with the MUMPS sparse direct solver. The actual implementation in the present study concerns the computation of the local contribution to the sub-matrix \hat{K}_{22} (second variation) and its corresponding vector of internal forces (first variation). Since the B2000++ FE code has an object-oriented architecture, these tasks are handled by a dedicated (nonlinear) boundary condition object. This boundary condition is also responsible for computing the kinematic coupling operator and its derivatives C , as well as for the reduction of the local degrees of freedom. To the nonlinear solver, such a boundary condition is an opaque object which, given a vector of d.o.f., returns a vector of forces, and its derivatives, the tangent stiffness matrix.

The local FE models are stored in a single separate database, which is accessed by the boundary condition to read the nodes, connectivities, material properties, additional boundary conditions, etc. To avoid re-implementation of these tasks, the existing (FE) model and solver classes of B2000++ are re-used inside the boundary condition.

3 Modal analysis via sub-structuring and reduction

3.1 Methodology

The computational effort of time-integration analysis is proportional to the number of different sets of initial conditions and loading conditions; this number is in general much higher for dynamic analysis than for static analysis. Thus, in industry, dynamic sub-structuring and reduction methods are preferred over a detailed FE analysis. While the computation of the reduced models can be time-consuming, their time-integration is fast, resulting in a considerable decrease of the overall computational effort.

In the following, a sub-structuring technique based on modal analysis is presented. **(1):** A complex structure is divided into several substructures (components). The analysis of each component can be assigned to different groups and/or computers. Hence, parallel processing opportunities are highly supported, **(2):** The number of d.o.f. in a large FE model is reduced significantly while the accuracy of the analysis is preserved within a low frequency range, **(3):** Analyses of component models are independent of each other. When modifications are required in a certain component, only reanalyzing this part is sufficient to determine the modified matrices of the structure. The unmodified substructures do not have to be analyzed again, **(4):** It is possible to use one parametric FE model for all the similar substructures. Thus, for structures consisting of repetitive components, generating the complete model

is not necessary. Depending on the type of the boundary conditions applied on the component interface nodes, Component Mode Synthesis (CMS) can be grouped into fixed interface methods Craig and Bampton (1968); Hurty (1965), free interface methods Goldman (1969); Mac Neal (1971); Rixen (2002); Rubin (1975) and loaded interface methods Benfield and Hrudá (1971). In this research, a fixed interface method, the Craig-Bampton (CB) (Craig and Bampton, 1968), is used for this purpose. Moreover, it is combined with an Interface Reduction (IR) methodology (Craig and Chang, 1977) to reduce the size of the CB based FE model even further.

After dividing the FE model of the complete structure into non-overlapping substructure FE models, the next step is the condensation of these models. In the CB method, this is achieved by projecting the substructure system matrices into a smaller subspace using the fixed interface normal modes, and the constraint modes. The first set of modes describes the internal dynamic behavior of a substructure. These are calculated by restraining all d.o.f. at the component interface and solving an undamped free vibration problem. The motion on the substructure interfaces, the propagation of the forces between substructures and the necessary information about the rigid body motions are defined via the constraint modes. These modes are calculated by statically imposing a unit displacement to the interface d.o.f. one by one while keeping the displacements of the other interface d.o.f. zero and assuming that there are no internal reaction forces.

Coupling of the CB substructure models requires both compatibility and force equilibrium to be satisfied at the interfaces of the components. The coupled system of equations of a CB model are obtained via a primal formulation. This formulation is based on defining a unique set of interface d.o.f. and eliminating the interface forces using the equilibrium on the interface. Finally, the modal analysis is performed on the coupled reduced system matrices.

While the number of internal substructure d.o.f. can be reduced with a significant amount, the number of interface d.o.f. is preserved in the CB model. The number of interface d.o.f. is therefore a bottleneck in the computational efficiency of CB, especially when the number of substructures or the interface d.o.f. is high. The Interface Reduction (IR) method is developed for the purpose of solving this issue. The idea behind the method is statically condensing a structure on its interface, performing an eigenvalue analysis on the condensed model to compute a truncated number of modes and finally utilizing them as a basis to reduce the number of interface d.o.f. The IR method is very effective in condensing the CB model while maintaining a certain accuracy.

3.2 Implementation in B2000++

The Craig-Bampton method is implemented into B2000++ via an FE solver which takes the finite element models of substructures as database inputs and writes the corresponding reduction basis and the reduced matrices into the database. Thus, the FE model of the entire domain is composed of a set of super elements which utilize the substructure reduced matrices as their stiffness and mass matrices. A sparse linear solver is employed to obtain the reduction basis and consequently, these matrices. Since the super elements involve all the interface d.o.f. of the corresponding substructures, their coupling is the same as that of the elements in the classic FE theory.

The implementation of the IR method is done using a boundary condition component which locks the generalized d.o.f. of the super elements. A free vibration analysis of the entire model, composed of the super elements and this boundary condition, gives the interface reduction basis. This reduction basis can then be used for further reduction in the CB model.

4 Demonstration of the concepts

The introduced concepts are demonstrated on a carbon fiber reinforced panel stiffened via three I-section stringers with tapered feet. The structure is clamped at the edges parallel to the y -axes. Each stringer is manufactured from four laminates; two of these laminates form the C-sections back-to-back, the third laminate forms the tapered base and the fourth laminate is placed on the top, see Figure 5.

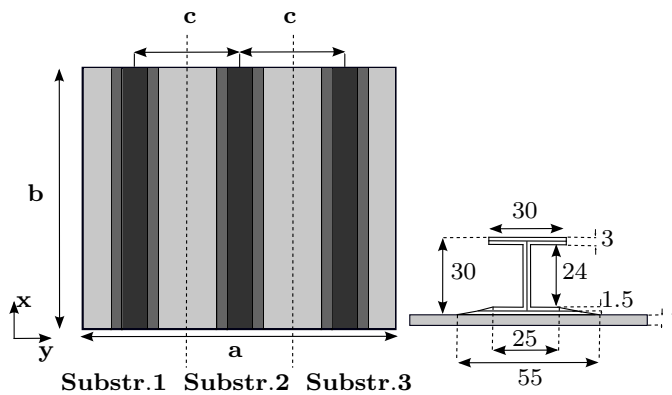


Figure 5: Test problem. Carbon fiber reinforced panel stiffened via three I-section stringers with tapered feet. The dimensions of the panel are $a = 360\text{mm}$, $b = 300\text{mm}$, $c = 120\text{mm}$, $t = 4\text{mm}$.

In addition, both the shape and the dimensions of the panel and the stringer are summarized in Figure 5. The panel is manufactured from a typical aerospace material, i.e. Hexcel T800/924. The composite lay up is created from the stacking sequence $[(+45^\circ / -45^\circ / 0^\circ / 90^\circ)_4]_s$. The laminate lay up of each stringer is $[(-45^\circ / +45^\circ / 0^\circ)_4]_s$. The orientations at 0° and 90° correspond to the x-axis and y-axis, respectively. The material properties of T800/924 are: The elastic moduli are $E_{11} = 155GPa$, $E_{22} = 8.57GPa$, Poisson's ratio is $\nu_{12} = 0.33$, Shear modulus is $G_{12} = 7.4GPa$ and the ply thickness is $0.125mm$. The remaining material properties are chosen as $E_{22} = E_{33} = 8.57GPa$, $\nu_{12} = \nu_{13} = 0.33$, $\nu_{23} = 0.052$, $G_{13} = G_{23} = 7.4GPa$ and the density $\rho = 1630kg/m^3$. The FE analyses are carried out using shell elements for the global model and 3D volume elements for the local models. The strain calculated for shell and volume models is the Green-Lagrange strain and the stress is the Cauchy stress.

The nonlinear static and modal analyses are carried out with the B2000++ FE code. All global and local FE models are generated with the sub modelling framework.

4.1 Global-Local analysis and tight two-way coupling methodology

Critical areas within the panel are determined during a preliminary non-linear static analysis. The edges of the panel parallel to the x-axis (Figure 5) are unconstrained. The structure is compression loaded via an incremental displacement load applied at the top side of the plate parallel to the y-axis (Figure 5). The displacement load is stepwise increased up to a value of $-2.00mm$. Approximately 2000 shell elements are used within the global FE model to mesh the geometry. The reference model used to compare the global-local result is meshed via 15000 3D volume elements.

Local models consisting of 3D volume elements are generated in regions of the shell element model where the failure index exceeds 0.57. Hence, 43 percent of the strength of the element in this region is left. The global-local approach is compared to a reference model created with 3D volume elements. In both models the failure index is determined via a Hashin(Hashin, 1980) failure criterion. Additional parameters necessary for this failure criterion are presented in Table 1. The results for the reference volume model and global-local model are shown in Figure 6.

Inclusion of the local models is limited to the region in between the stiffeners, see Figure 6(a) bottom and (b) bottom. High failure indices at the clamped edges are due to introducing the loading. Between the stiffeners a non-symmetric displacement pattern typical for this buckled plate is visible. Hence, the skin left to the central stiffener buckles before the right part of the plate. Here, strains are high and a 3D volume model is inserted to predict the remaining strength of the material. The bottom Figure 6(a) and (b) show the global-local models are created in the areas where high failure indices are computed. These areas are similar to the

Table 1: Material properties used for the different failure criteria.

parameters	Hashin(Hashin, 1980)
maximum tension fiber direction	1982.0 MPa
maximum tension orthogonal to fiber direction	48.69 MPa
maximum compression fiber direction	1550.0 MPa
maximum compression orthogonal to fiber direction	250.0 MPa
maximum shear strength	113.0 MPa
maximum shear strength	113.0 MPa
maximum shear strength	113.0 MPa

high failure index areas in the reference model, see Figure 6(a) and (b). Because the global shell element model uses far less elements than the reference model the region with high failure indices is larger in the shell element model. However, the magnitude of the computed failure index in both the reference model and the global-local model are comparable.

During the global-local analysis with Hashin failure criterion no numerical difficulties were observed with respect to the convergence of the incremental loading steps. In addition, the insertion of local models at the boundaries of the global model did not pose any difficulties. The boundary conditions are applied on the global model only and automatically accounted for in the local model. Furthermore, no stress jumps were observed at the interfaces of the global and global-local region. However, the computational effort required to perform the static condensation of the local models is significant. Therefore, future research will focus on improving numerical performance to enable up-scaling of the method to larger global models, e.g. barrel sections.

4.2 Analysis via sub-structuring and reduction methods

The complete structure is divided into three identical components. Each component consists of one third of the panel and a single stringer, see Figure 5. The coarse global (full) and the reduced models are generated utilizing the model of a single substructure.

The size of the full (global) and the reduced FE models and, the number of the reduction components are summarized in Table 2. For each substructure 18 fixed interface normal modes are utilized. There exist 25 unconstrained nodes on each interface that contribute to the constraint modes of each component. Depending on

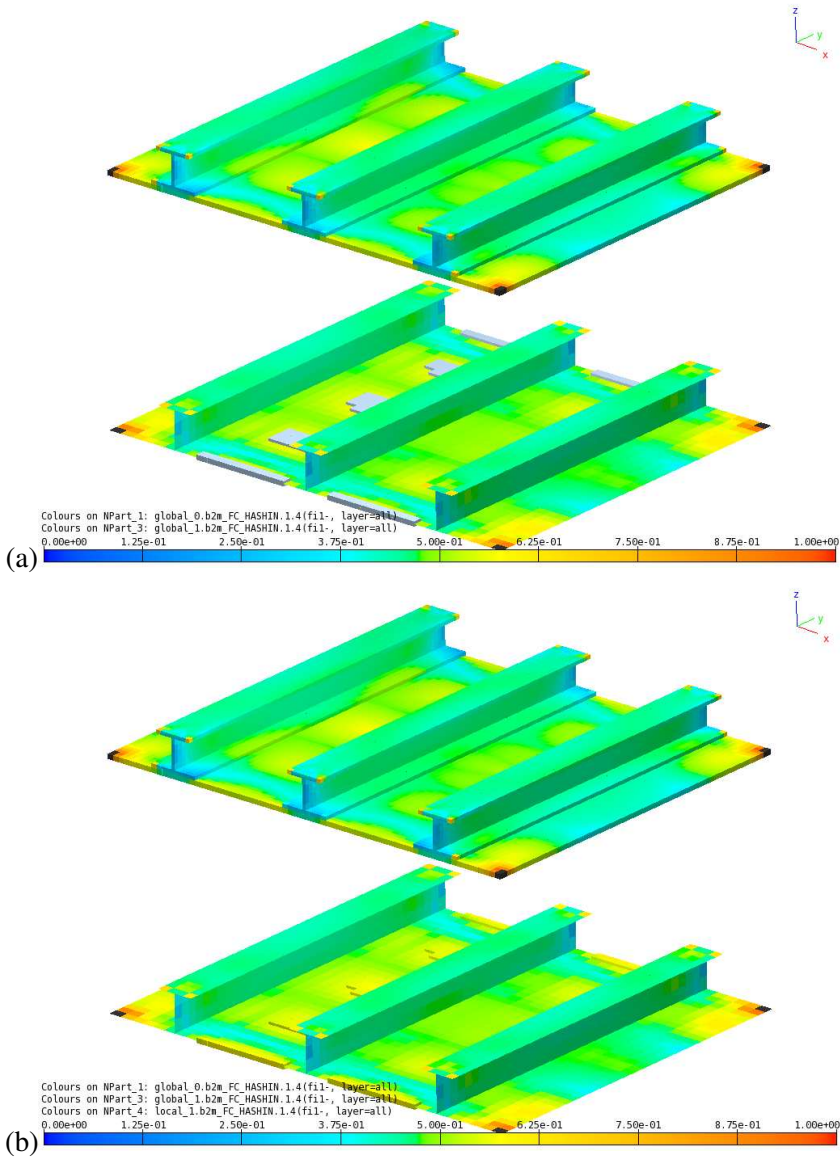


Figure 6: Failure index of a compression loaded stiffened plate modelled via volume elements ((a) and (b) top) or modelled via local volume models superimposed onto a global shell element mesh ((a) and (b) bottom). In Figure (a) the local models are grey for clarity. In Figure (b) the local models are colored with the computed failure index. Inclusion of local models is limited to the region in between the stiffeners.

the number of utilized IR basis, it is possible to reduce the total interface d.o.f. of the complete structure from 300 d.o.f. to 6, 12, 18, 20 d.o.f. as shown in Table 2. Accordingly, the original system matrices can be condensed significantly using the CB and the CB&IR methods.

Table 2: The number of d.o.f. and the reduction components

Method	# of Fixed Interface Modes (per substructure)	# of d.o.f. on each interface	# of IR basis	# of d.o.f.
Full (Global) Model	-	-	-	12456
Craig-Bampton (CB)	18	150	-	354
CB&IR ₆	18	-	6	60
CB&IR ₁₂	18	-	12	66
CB&IR ₁₈	18	-	18	72
CB&IR ₂₀	18	-	20	74

The accuracy of the reduction methods are computed on the basis of the relative frequency error (ϵ_ω) and the Modal Assurance Criterion (MAC). ϵ_ω is calculated using the full FE results and comparing them with the results of the IR and the CB methods using

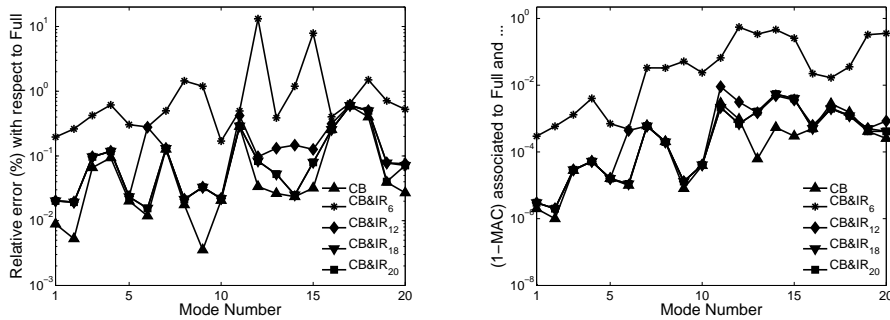
$$\epsilon_\omega = \frac{|[\Lambda_{Full}]_{jj}^{\frac{1}{2}} - [\Lambda_R]_{jj}^{\frac{1}{2}}|}{[\Lambda_{Full}]_{jj}^{\frac{1}{2}}} 100 \quad j = 1, \dots, 20$$

where “R” represents the reduction method, $|\cdot|$ is the absolute value and Λ_{jj} is the j th diagonal entry of the spectral matrix Λ . It is important to note that the formula defines the percentage error (%). MAC is a scalar value between 0 and 1, and it represents the correlation number between the two mode shapes. A MAC value close to 1 indicates a high degree of correlation between two mode shapes. For its calculation, first the reduced model solutions are expanded to their full forms and then these eigenvectors are compared with the eigenvectors calculated by full FE analysis using

$$MAC = \frac{([\tilde{\Phi}_{Full}]_j^T [\tilde{\Phi}_R]_j)^2}{([\tilde{\Phi}_{Full}]_j^T [\tilde{\Phi}_{Full}]_j)([\tilde{\Phi}_R]_j^T [\tilde{\Phi}_R]_j)} \quad j = 1, \dots, 20 \tag{6}$$

where $[\check{\Phi}_{Full}]_j, [\check{\Phi}_{IR}]_j$ are the j th eigenvectors corresponding to the full FE analysis and the reduction method, respectively.

The results of the test problem are presented in Figure 7.



(a) Relative errors of frequencies with respect to the Full FE results (b) Correlation of the mode shapes with the Full FE results

Figure 7: Results of the CB and the IR methods

The accuracy of the CB method is in good agreement with the reference values and, the utilized d.o.f. are significantly less than those of the global FE method. The maximum relative error among the first twenty natural frequencies with respect to the full FE results is less than 1%. In addition, the computed mode shapes show a good correlation with the global FE results.

Further reduction in the CB model is obtained by employing Interface Reduction (IR) methodology. The IR model with 6 basis vectors is in good agreement with the reference values up to the 7th natural frequency. The results show that for increasing number of basis vectors the solutions converge to the CB results. The accuracy of the computed first 20 eigenvalues and the corresponding frequencies are in good agreement with the reference values for the IR model with 18 basis vectors. The number of d.o.f. in this model is 173 times less than that of the global model. The results clearly show it is possible to accomplish a significant reduction of the size of the global model while preserving an acceptable degree of accuracy for modal analysis problems.

5 Conclusions and future work

The automated approach to generate different fidelity models with a single modelling and meshing toolkit was found efficient and time saving. In addition, boundary conditions applied to the analysis model for non-linear static analysis did not

require additional efforts from the user and were naturally accounted for. Similarly good analysis results were obtained via the linear dynamic sub structuring and reduction modal analysis. However, the static condensation of the local models that is applied for non-linear static global-local analysis was found to be computationally demanding and requiring further research to speed up this step in the computations. The research presented in this paper is part of a larger ongoing effort to automatically generate different FE fidelity models within a single design platform. This platform handles the communication between the different fidelity models and the exchange of analysis results. Therefore, user interaction to analyze a structure for different analysis cases is reduced to a minimum. The carbon-fiber stiffened panel is a suitable example in this context. It contains all the relevant characteristics of an industrial use case.

Acknowledgement

The authors wish to acknowledge Mathias Doreille¹ for his suggestions and support. The authors would like to thank the anonymous reviewers for their valuable comments to help improve the quality of the paper. Part of the research leading to these results was carried out within the project "generic linking of Finite Element based Models - glFEM" which has received funding from the European Community's Seventh Framework Programme (FP7/2007-2013) under grant agreement no 234147.

References

- Amestoy, P. R.; Duff, I. S.; Koster, J.; L'Excellent, J.-Y.** (2001): A fully asynchronous multifrontal solver using distributed dynamic scheduling. *SIAM Journal on Matrix Analysis and Applications*, vol. 23, no. 1, pp. 15–41.
- Amestoy, P. R.; Guermouche, A.; L'Excellent, J.-Y.; Pralet, S.** (2006): Hybrid scheduling for the parallel solution of linear systems. *Parallel Computing*, vol. 32, no. 2, pp. 136–156.
- Benfield, W.; Hruda, R.** (1971): Vibration analysis of structures by component mode substitution. *AIAA*, vol. 9, no. 7, pp. 1255–1261.
- Craig, R. R.; Bampton, M. C. C.** (1968): Coupling of substructures for dynamic analysis. *AIAA*, vol. 6, no. 7, pp. 1313–1319.
- Craig, R. R.; Chang, C. J.** (1977): Substructure coupling for dynamic analysis and testing. Technical report, NASA, CR-2781, 1977.

¹ SMR Engineering and & Development, Switzerland, doreille@smr.ch

- Fish, J.; Shek, K.** (2000): Multiscale analysis of large scale nonlinear structures and materials. *International Journal for Computational Civil and Structural Engineering*, vol. 1, pp. 79–90.
- Goldman, R.** (1969): Vibration analysis by dynamic partitioning. *AIAA*, vol. 7, pp. 1152–1154.
- Hashin, Z.** (1980): Failure criteria for unidirectional fiber composites. *Journal of Applied Mechanics*, vol. 47, pp. 329–334.
- Hund, A.** (2007): *Hierarchische mehrskalennmodellierung des versagens von werkstoffen mit mikrostruktur*. PhD thesis, Universitaet Stuttgart, 2007.
- Hurty, W.** (1965): Dynamic analysis of structural systems using component modes. *AIAA*, vol. 3, no. 4, pp. 678–685.
- Mac Neal, R.** (1971): A hybrid method of component mode synthesis. *Computers and Structures*, vol. 1, no. 4, pp. 581–601.
- Python Software Foundation** (2012): Python, 2012.
- Rixen, D.** (2002): A dual Craig-Bampton method for dynamic substructuring. *Journal of Computational and Applied Mathematics*, vol. 168, no. 1-2, pp. 383–391.
- Rubin, S.** (1975): Improved component mode representation for structural dynamic analysis. *AIAA*, vol. 13, no. 8, pp. 995–1006.